IEEE Access
Multidisciplinary | Rapid Review | Open Access Journal

Received March 1, 2019, accepted March 11, 2019, date of publication March 15, 2019, date of current version April 1, 2019.

Digital Object Identifier 10.1109/ACCESS.2019.2905265

Sequential Multi-Sensor JPDA for Target Tracking in Passive Multi-Static Radar With Range and Doppler Measurements

XIAOYONG LYU[1] AND JUN WANG[2]
[1]School of Information Engineering, Zhengzhou University, Zhengzhou 450001, China
[2]National Laboratory of Radar Signal Processing, Xidian University, Xi'an 710071, China

Corresponding author: Xiaoyong Lyu (iexyl@zzu.edu.cn)

This work was supported by the National Key Laboratory of Science and Technology on Space Microwave, China, under Grant 614241103030617.

ABSTRACT Target tracking in passive multi-static radar (PMSR) with bistatic range and Doppler frequency measurements from multiple transmit–receive pairs is gaining increasing interest. For the data association problem in this scenario, the parallel architecture of a multi-sensor joint probabilistic data association (P-MSJPDA) filter has been significantly investigated. As an alternative architecture, the sequential MSJPDA (S-MSJPDA) is rarely discussed in PMSR. In this paper, we evaluate the behaviors of S-MSJPDA in PMSR target tracking with bistatic range and Doppler frequency measurements. A comprehensive comparison between the S-MSJPDA and the P-MSJPDA in PMSR is provided. It can be found from the analysis that S-MSJPDA outperforms its parallel counterpart in terms of computational efficiency, given an acceptable degradation in position accuracy. The S-MSJPDA is further applied to an experimental passive multi-static radar for aircrafts tracking. The real data results obtained are rather close to the true trajectories of the targets. This demonstrates that the S-MSJPDA has great potentials in PMSR target tracking.

INDEX TERMS Passive multi-static radar, target tracking, multi-sensor joint probabilistic data association.

I. INTRODUCTION

Over the last two decades, passive radar has received a renewed interest for civilian and military applications [1], [2]. Passive radar exploits existing transmitters as illuminators of opportunity; thus it needs neither frequency allocation nor extra hardware, and the detection of targets is covert, continuous, and also inexpensive [3]–[9]. Specifically, when more than one transmitter is simultaneously exploited, a passive multi-static radar (PMSR) is formed. In this case the location and trajectory of a potential target can be determined by combining measurements from multiple transmit–receive pairs with overlapping coverage. This provides the PMSR with great potentials in air surveillance [10]–[13]. The measurements available in PMSR for target tracking are usually bistatic range, Doppler frequency and direction of arrival (DOA). In many passive radar systems, DOA is hard to get with satisfactory accuracy, especially for those equipped with small antennas. The poor quality of DOA usually results in great degradation in the estimation accuracy of a target's trajectory [14], [15]. Therefore, tracking with only bistatic range and Doppler frequency in PMSR is attracting increasing attention.

Target tracking in PMSR is a typical multi-sensor multi-target tracking problem. In this situation [16], measurements may originate from one of the various targets whose existence and trajectories are not known a priori, as well as from other random sources, which are usually termed as clutter. In addition, target measurements are only present in a scan with some probability of detection $P_D < 1$. Targets may enter and leave the surveillance region at any time, thus at any given moment the number of targets in the surveillance area is unknown. More challengingly in PMSR with only range and Doppler measurements, the position of a target cannot be determined by using only one transmit-receive pair. To cope with these difficulties, research has been conducted on track initiation, track confirm, track maintenance, and track terminate [17]–[20]. In this paper we assume track initiation and confirm to have been performed beforehand. We only focus on track maintenance, where we will evaluate the behaviors of S-MSJPDA in PMSR, and compare with that of P-MSJPDA, which has rarely been discussed previously.

In the following we give a review of the multi-sensor multi-target tracking methods. These methods can be

The associate editor coordinating the review of this manuscript and approving it for publication was Guan Gui.

classified into two categories, i.e. association-based methods and non-association methods [21], [22]. The association-based methods usually involve measurement-to-track association and may be grouped into two types, i.e. non-Bayesian methods and Bayesian approaches. The non-Bayesian methods include the greedy nearest-neighbor filter and the multi-dimensional assignment method. The greedy nearest-neighbor filter assigns a target with the measurement that is closest to the predicted position of the target [23]. In dense target or clutter scenario, the closest measurement is usually not the true measurement from the target, so the nearest-neighbor filter degrades severely in this case. The multi-dimensional assignment method finds the best measurement-target association by posing it as a multi-dimensional assignment problem [24]. Optimal implementation of multi-dimensional assignment is NP-hard and some approximation schemes should be invoked, such as Lagrangian relaxation techniques [25]. The Bayesian approaches include the multi-hypothesis tracker (MHT) and the JPDA filter [26], [27]. MHT enumerates the measurement to target association hypothesis using measurements from all the scans. The hypothesis with the highest posterior is returned as a solution. JPDA formulates measurement-target associations and computes the association probabilities by exploiting the measurements only from the current scan. Given an association, the state of a target is estimated by a filtering algorithm and this conditional state estimate is weighted by the association probability. Then the state of a target is estimated by summing over the weighted conditional estimates. Optimal MHT and JPDA consume excessive time, since the number of association hypothesis increases exponentially with the number of targets and measurements. Pruning schemes are usually adopted to reduce the hypothesis number [28]–[30].

The most representative non-association methods are those based on finite-set statistics (FISST), which provides a set of mathematical tools that extends the Bayesian filtering framework to the multi-target tracking problems [31]. This avoids explicit measurement-to-track associating. The optimal implementation of multi-target tracking based on FISST is computational intractable, because the propagation of the multi-target posterior involves the evaluation of multiple set integrals. A more tractable alternative is the probability hypothesis density (PHD) filter which propagating the first moment associated with the multi-target posterior [32]–[34].

It is hard to assert which of the two categories is better, but one statement is often mentioned in the literatures. That is the association-based methods are readily to cause ghost targets which can be handled by the non-association methods at the cost of requiring more computation [35].

As for multi-target tracking in PMSR with bistatic range and Doppler frequency measurements, the MSJPDA framework has been widely used and verified. It is known that there are two implementation architectures of MSJPDA [36], i.e. P-MSJPDA and S-MSJPDA. The P-MSJPDA exploits all measurements from all the sensors simultaneously to update the tracks of potential targets. Most of the PMSR multi-target tracking methods are based on the P-MSJPDA, such as those in [37]–[39] developed for target tracking in digital audio/video broadcasting (DAB/DVB) passive radar. The disadvantage of P-MSJPDA is that the multi-sensor data associating consumes excessive time. The S-MSJPDA is to process the measurements sensor by sensor. That is, it first exploits the measurements from the first senor to update the tracks of the targets, and then the measurement from the second sensor. Repeat this process until the measurements from the last sensor are processed. S-MSJPDA breaks the multi-sensor data association problem into several single-sensor data association problems, of which the treatment is more efficient. Intuitively, S-MSJPDA has great potentials in target tracking. But it is rarely discussed in PMSR. In this paper we evaluate the behaviors of S-MSJPDA in PMSR target tracking with bistatic range and Doppler frequency measurements, and give a comprehensive comparison between the two architectures. It should be noted that the optimal implementations of the both methods are NP-hard, and there is no practical value to compare two algorithms with intractable computation. In this paper the near optimal approximations of the both architectures are proposed based on the m-best assignment technique. The comparison is conducted over the approximation versions. Theoretical analysis of the computational complexity of the both methods is conducted. It will be found from the later analysis that the S-MSJPDA is more efficient than P-MSJPDA because the association event in S-MSJPDA is simpler, of which the association probabilities is easier to be computed. However, S-MSJPDA degrades in position accuracy compared to P-MSJPDA owing to the approximation strategies used in the both methods. Fortunately, this degradation is rather small and therefore acceptable. The S-MSJPDA is further verified by real experiments for aircrafts tracking. An experimental frequency modulation (FM) based PMSR is utilized for the experiments. The real data results are presented and analyzed. More details can be found in the paper below.

The organization of the paper is as follows. Section I gives the introduction. Section II gives the target tracking problem definition in PMSR with bistatic range and Doppler frequency measurements. Section III introduces the framework of MSJPDA. The derivations of P-MSJPDA and S-MSJPDA are presented, with emphasis on the near optimal implementation strategies of the both architectures. The computational complexity of the both methods are analyzed theoretically. Section IV provides a comprehensive comparison between the behaviors of the both methods through simulations. Section V gives the experimental validation of the S-MSJPDA. The experiment setup and the FM-based PMSR configuration are introduced. The real data results are presented and analyzed. Section VI gives the conclusions.

II. TARGET TRACKING PROBLEM DEFINITION

Consider a PMSR configuration depicted in figure 1. N signal transmitters located in different positions are adopted as the illuminators of opportunity. One radar receiver is deployed

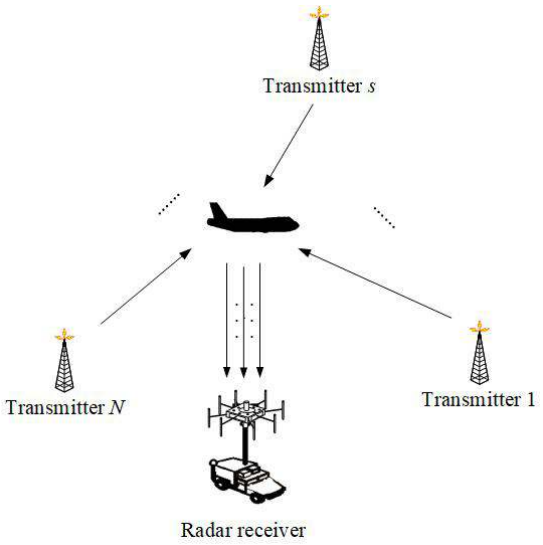

FIGURE 1. PMSR configuration.

to receive and process target echoes. We assume in the paper that signals from different transmitters are resolvable. This is applicable for many communication signals such as the FM and many satellite signals [14], [40], [41].

A. TARGET MODEL

In this paper we are interested in tracking K slowly maneuvering targets, and we ignore the altitudes of the targets as many other passive radars although the methods presented in the paper can be easily extended to 3-dimension tracking scenario. The state of the τ-th target comprises its position $\mathbf{p}^\tau(k) = [x^\tau(k), y^\tau(k)]^T$ and velocity $\mathbf{v}^\tau(k) = [\dot{x}^\tau(k), \dot{y}^\tau(k)]^T$, i.e.

$$\mathbf{x}^\tau = [x^\tau(k), \dot{x}^\tau(k), y^\tau(k), \dot{y}^\tau(k)]^T$$

Assuming further a uniform discretization with a sampling period of T_s seconds, the state evolution equation for the τ-th target becomes:

$$\mathbf{x}_k^\tau = \mathbf{F}_k \mathbf{x}_{k-1}^\tau + \mathbf{w}_k \tag{1}$$

where:

$$\mathbf{F}_k = \begin{bmatrix} 1 & T_s & 0 & 0 \\ 0 & 1 & 0 & 0 \\ 0 & 0 & 1 & T_s \\ 0 & 0 & 0 & 1 \end{bmatrix}$$

$\mathbf{w}_k$ is the process noise following a zero mean Gaussian distribution with the covariance matrix:

$$\mathbf{Q} = \begin{bmatrix} \frac{1}{4}T_s^4 & \frac{1}{2}T_s^3 & 0 & 0 \\ \frac{1}{2}T_s^3 & T_s^2 & 0 & 0 \\ 0 & 0 & \frac{1}{4}T_s^4 & \frac{1}{2}T_s^3 \\ 0 & 0 & \frac{1}{2}T_s^3 & T_s^2 \end{bmatrix}$$

The collection of tracks in time k is denoted by $\mathbf{x}_k = \{\mathbf{x}_k^1, \mathbf{x}_k^2, \ldots, \mathbf{x}_k^K\}$.

B. MEASUREMENT AND SENSOR MODEL

In this paper we consider collecting the bistatic range and Doppler frequency measurements in PMSR to determine the track of a target. We call a transmit-receive pair in the PMSR as a sensor hereafter. The target measurement of each sensor at time k is modeled as:

$$\mathbf{y}_{s,k}^\tau = \begin{bmatrix} \gamma_s^\tau \\ f_{d,s}^\tau \end{bmatrix} = \mathbf{h}_s(\mathbf{x}_k^\tau) + \boldsymbol{\upsilon}_{s,k},\ s=1,2,\ldots,N \tag{2}$$

where γ_s^τ and $f_d^{s,\tau}$ are the bistatic delay and Doppler frequency of target τ measured by sensor s. $\boldsymbol{\upsilon}_{s,k}$ is the measurement noise following a zero-mean white Gaussian distribution with covariance matrix $\mathbf{R}_k$.

$$\mathbf{h}_s(\mathbf{x}_k^\tau) = \begin{bmatrix} \frac{R_{tran,s}^\tau + R_{rec}^\tau}{c} \\ -\frac{f_{c,s}}{c}\mathbf{v}^\tau(k)^T\left(\frac{\mathbf{p}^\tau(k) - \mathbf{p}_{tran,s}}{R_{tran,s}^\tau} + \frac{\mathbf{p}^\tau(k) - \mathbf{p}_{rec}}{R_{rec}^\tau}\right) \end{bmatrix} \tag{3}$$

$$R_{rec}^\tau = \sqrt{(x^\tau(k)\text{-}x_{rec})^2 + (y^\tau(k)\text{-}y_{rec})^2} \tag{4}$$

$$R_{tran,s}^\tau = \sqrt{(x^\tau(k)\text{-}x_{tran,s})^2 + (y^\tau(k)\text{-}y_{tran,s})^2} \tag{5}$$

c is the velocity of light, $\mathbf{p}_{tran,s} = [x_{tran,s}, y_{tran,s}]^T$ is the position of the s-th transmitter, and $\mathbf{p}_{rec} = [x_{rec}, y_{rec}]^T$ is the position of the receiver.

The collection of measurements at sensor s including clutter at time k is represented as $\mathbf{y}_{s,k} = \{\mathbf{y}_{s,k}^1, \mathbf{y}_{s,k}^2, \ldots, \mathbf{y}_{s,k}^K\} \bigcup \mathbf{c}_{s,k}$, where $\mathbf{c}_{s,k}$ is the set of clutter measurements obtained by the s-th sensor. It is noted that some targets may not be detected by sensor s at time k, so the corresponding notations should be removed from $\mathbf{y}_{s,k}$. The measurement collection of sensor s up to and including time$k$ is denoted by $\mathbf{Y}_s^k$, $s = 1, 2, \ldots, N$, then we have $\mathbf{Y}_s^k = \mathbf{y}_{s,k} \bigcup \mathbf{Y}_s^{k-1}$, $s = 1, 2, \ldots, N$. The number of measurements at each sensor varies with time, and it is usually different from the number of true targets. We assume that each of the targets can generate at most one measurement per sensor at a particular time instant, and each of the measurements per sensor can originate from at most one target. However, several measurements may be due to clutter.

To address the data association problem, it is necessary to introduce association events, each of which is a complete assignment of measurements to targets or clutter. We add a dummy track denoted by $\mathbf{x}_k^0$ in the track set $\mathbf{x}_k$ and a dummy measurement $\mathbf{y}_{s,k}^0$ in each measurement set $\mathbf{y}_{s,k}$. Define an association variable $\mathbf{Z}_{\tau,i_1,\ldots,i_N} = [\tau, i_1, \ldots, i_N]$, which claims that measurements $\mathbf{y}_{1,k}(i_1), \ldots, \mathbf{y}_{N,k}(i_N)$ originate from target τ ($0 \le \tau \le K$), where $\mathbf{y}_{s,k}(i_s)$ is the i_s-th measurement in measurement set $\mathbf{y}_{s,k}$ and $0 \le i_s \le n_s$. n_s is the total number of measurements in $\mathbf{y}_{s,k}$. It is noted that $\tau = 0$ means that $\mathbf{y}_{1,k}(i_1), \ldots, \mathbf{y}_{N,k}(i_N)$ are all due to clutter. $i_s = 0$ means that no measurements at sensor s are due to

target τ. A complete association event $\boldsymbol{\theta}$ includes a set of association variables $[(\mathbf{Z}^{(1)}_{\tau,i_1,\ldots,i_N})^T,\ldots,(\mathbf{Z}^{(L)}_{\tau,i_1,\ldots,i_N})^T]$, such that measurements at each sensor are assigned to corresponding targets or claimed as clutter, conditioned on the assumption that each measurement per sensor originates from at most one target and that each target generates at most one measurement per sensor:

$$\boldsymbol{\theta} = \begin{bmatrix} \mathbf{Z}^{(1)}_{\tau,i_1,\ldots,i_N} \\ \mathbf{Z}^{(2)}_{\tau,i_1,\ldots,i_N} \\ \vdots \\ \mathbf{Z}^{(L)}_{\tau,i_1,\ldots,i_N} \end{bmatrix} = \begin{bmatrix} \tau^{(1)}, i^{(1)}_1,\ldots,i^{(1)}_N \\ \tau^{(2)}, i^{(2)}_1,\ldots,i^{(2)}_N \\ \vdots \\ \tau^{(L)}, i^{(L)}_1,\ldots,i^{(L)}_N \end{bmatrix}$$
$$\tau^{(l)} \neq \tau^{(j)}, \text{for} l \neq j, \tau^{(l)} \neq 0, \text{and} \tau^{(j)} \neq 0$$
$$i^{(l)}_s \neq i^{(j)}_s, \text{for} l \neq j, i^{(l)}_s \neq 0, \text{and} i^{(j)}_s \neq 0 \quad (6)$$

The subscript (j) in (6) is used to discriminate between different association variables, and it will be omitted to avoid the symbol abuse in the following if ambiguity is not induced. It can be seen in the association matrix that the combination between column 1 and column $s+1$ denoted by $\boldsymbol{\varepsilon}_s$ is an association event that assigns each measurement at sensor s to a target or claims it as clutter:

$$\boldsymbol{\varepsilon}_s = \begin{bmatrix} \mathbf{Z}^{(1)}_{\tau,i_s} \\ \mathbf{Z}^{(2)}_{\tau,i_s} \\ \vdots \\ \mathbf{Z}^{(L)}_{\tau,i_s} \end{bmatrix} = \begin{bmatrix} \tau^{(1)}, i^{(1)}_s \\ \tau^{(2)}, i^{(2)}_s \\ \vdots \\ \tau^{(L)}, i^{(L)}_s \end{bmatrix}$$

III. MULTI-SENSOR JPDA

In this section we first introduce the MSJPDA framework and then give the derivations of P-MSJPDA and S-MSJPDA, with emphasis on the near optimal implementation strategies of the both architectures. Theoretical analysis of the computational complexity of the both methods is also presented.

Instead of maintaining the posterior probability density of the joint state $p(\mathbf{x}_k|\mathbf{Y}^k)$, the JPDA updates the marginal density for each target $p(\mathbf{x}^\tau_k|\mathbf{Y}^k)$, $\tau = 1, 2, \ldots, K$ through the Bayesian sequential estimation recursion, which effectively combats the curse of dimensionality. For the multi-sensor case we described above, the posterior density of target τ given measurements at all the sensors can be written as follows:

$$p(\mathbf{x}^\tau_k|\mathbf{Y}^k_1,\ldots,\mathbf{Y}^k_N) = \sum_{\boldsymbol{\theta}} p(\boldsymbol{\theta}|\mathbf{Y}^k_1,\ldots,\mathbf{Y}^k_N) p(\mathbf{x}^\tau_k|\boldsymbol{\theta},\mathbf{Y}^k_1,\ldots,\mathbf{Y}^k_N) \quad (7)$$

where $\boldsymbol{\theta}$ is the association event as described in section II. $p(\boldsymbol{\theta}|\mathbf{Y}^k_1,\ldots,\mathbf{Y}^k_N)$ is the posterior probability density of association event $\boldsymbol{\theta}$ conditioned on the measurements at the current instant, and:

$$p(\boldsymbol{\theta}|\mathbf{Y}^k_1,\ldots,\mathbf{Y}^k_N) \propto p(\mathbf{y}_{1,k},\ldots,\mathbf{y}_{N,k}|\boldsymbol{\theta},\mathbf{Y}^{k-1}_1,\ldots,\mathbf{Y}^{k-1}_N) \quad (8)$$

Actually, both P-MSJPDA and S-MSJPDA are designed to compute (7).

A. PARALLEL MSJPDA

Assuming a Gaussian distribution of $\mathbf{x}^\tau_k$, (7) can be represented as

$$p(\mathbf{x}^\tau_k|\mathbf{Y}^k_1,\ldots,\mathbf{Y}^k_N) = N(\mathbf{x}^\tau_k|\hat{\mathbf{x}}^\tau_k,\hat{\mathbf{P}}^\tau_k)$$

P-MSJPDA exploits all the measurements from all the sensors associated with target τ simultaneously to update the target state with the association probabilities

$$\hat{\mathbf{x}}^\tau_k = \sum_{s=1}^{N}\sum_{i_s=0}^{n_s} \beta^\tau_{i_s}\tilde{\mathbf{x}}^\tau_k(i_s)$$
$$\hat{\mathbf{P}}^\tau_k = \sum_{s=0}^{N}\sum_{i_s=0}^{n_s} \beta^\tau_{i_s}\left\{\tilde{\mathbf{P}}^\tau_k(i_s) + (\tilde{\mathbf{x}}^\tau_k(i_s)-\hat{\mathbf{x}}^\tau_k)(\tilde{\mathbf{x}}^\tau_k(i_s)-\hat{\mathbf{x}}^\tau_k)^T\right\} \quad (9)$$

where $\tilde{\mathbf{x}}^\tau_k(i_s)$ is the result of updating target τ by only using measurement $\mathbf{y}_{s,k}(i_s)$, and $\tilde{\mathbf{P}}^\tau_k(i_s)$ is the corresponding covariance matrix. Since the bistatic range and Doppler frequency equations in PMSR are non-linear, conventional Kalman filter (KF) is not applicable to compute the statistical quantities above [42]. This can be overcome with a non-linear filter such as the unscented Kalman filter (UKF) [43]. $\beta^\tau_{i_s}$ is the probability of associating measurement $\mathbf{y}_{s,k}(i_s)$ to target τ, and is the summation of the posterior probabilities of the association events $\boldsymbol{\theta}$ in which measurement $\mathbf{y}_{s,k}(i_s)$ is assigned to target τ

$$\beta^\tau_{i_s} \propto \sum_{\boldsymbol{\theta}} p(\boldsymbol{\theta}|\mathbf{Y}^k_1,\ldots,\mathbf{Y}^k_N) \quad (10)$$

where

$$p(\boldsymbol{\theta}|\mathbf{Y}^k_1,\ldots,\mathbf{Y}^k_N)$$
$$\propto \prod_{j=1}^{L} p(\mathbf{y}_{1,k}(i^{(j)}_1),\ldots,\mathbf{y}_{N,k}(i^{(j)}_N)|\mathbf{Z}^{(j)}_{\tau,i_1\ldots i_N},\mathbf{Y}^{k-1}_1,\ldots,\mathbf{Y}^{k-1}_N)$$
$$= \prod_{j=1}^{L}\prod_{s=1}^{N} p(\mathbf{y}_{s,k}(i^{(j)}_s))|\tau^{(j)},\mathbf{Y}^{k-1}_s) \quad (11)$$

$p(\mathbf{y}_{s,k}(i_s)|\tau,\mathbf{Y}^{k-1}_s)$ is the predicted measurement likelihood corresponding to target τ, and can also be easily obtained with UKF.

In order to compute the association probabilities $\beta^\tau_{i_s}$, the optimal MSJPDA enumerates all the association events $\boldsymbol{\theta}$, which is NP-hard especially for the multi-sensor case. In practice, many association events only have very low probabilities and contribute little to the solution. A practical and near optimal approximation is to select the m-best association events with the m-largest probabilities. Suppose $\boldsymbol{\theta}^{(1)},\boldsymbol{\theta}^{(2)},\ldots,\boldsymbol{\theta}^{(m)}$ are the m-best association events, thus (10) becomes

$$\beta^\tau_{i_s} \propto \sum_{1\leq i\leq m} p(\boldsymbol{\theta}^{(i)}|\mathbf{Y}^k_1,\ldots,\mathbf{Y}^k_N) \quad (12)$$

In the multi-sensor scenario we describe above, finding the m-best association events is a typical m-best $(N+1)$-D assignment problem, which can be solved within polynomial time. To formulate the m-best $(N+1)$-D assignment problem, each of the association event $\boldsymbol{\theta}$ is assigned with a cost measured as its generalized likelihood ratio, i.e.

$$c(\boldsymbol{\theta}) = \prod_{j=1}^{L}\prod_{s=1}^{N} \frac{p(\mathbf{y}_{s,k}(i_s^{(j)}))|\tau^{(j)}, \mathbf{Y}_s^{k-1})}{V_s} \tag{13}$$

where V_s is the volume of the view filed of sensor s. Let Ξ denote the association event space, which contains all the feasible association events $\boldsymbol{\theta}$. Then the m-best $(N+1)$-D assignment problem is casted in the following:

$$\begin{aligned}
\boldsymbol{\theta}^{(1)} &= \arg\min_{\boldsymbol{\theta}\in\Xi}\{c(\boldsymbol{\theta})\} \\
\boldsymbol{\theta}^{(2)} &= \arg\min_{\boldsymbol{\theta}\in\Xi\backslash\boldsymbol{\theta}^{(1)}}\{c(\boldsymbol{\theta})\} \\
&\vdots \\
\boldsymbol{\theta}^{(m)} &= \arg\min_{\boldsymbol{\theta}\in\Xi\backslash\boldsymbol{\theta}^{(n)}}\{c(\boldsymbol{\theta})\} \\
&\qquad n = 1, 2, \ldots, m-1
\end{aligned} \tag{14}$$

It is noted that each optimization problem in (14) represents a $(N+1)$-D assignment problem. Therefore, the m-best $(N+1)$-D assignment is accomplished by conducting several $(N+1)$-D assignments, each of which can be solved within a polynomial time by the successive Lagrangian relaxation technique in [44]. The worst-case complexity for computing (14) is $O(m(N+1)\rho L^4)$, where L is the number of the $(N+1)$-tuples in $\boldsymbol{\theta}$ and ρ is the number of relaxation iterations in a single $(N+1)$-D assignment. This complexity can further be reduced to $O(m(N+1)\rho L^3)$ with some preprocessing and optimization steps [45]. However, this complexity does not take into account the calculation of assignment cost $c(\boldsymbol{\theta})$, which still has a great complexity of $(K+1)\prod_{s=1}^{N}(n_s+1)$.

B. SEQUENTIAL MSJPDA

Instead of updating the probability density of target τ with the measurements at all sensors simultaneously, S-MSJPDA uses the measurements at different sensors sequentially. Suppose $\hat{\mathbf{x}}_{k-1}^{\tau}$ is the estimated state of target τ at the previous time instant, and $\hat{\mathbf{P}}_{k-1}^{\tau}$ is the covariance matrix. The sequential updating scheme is presented as follows.

Step 1: use measurements at sensor 1 to update $\hat{\mathbf{x}}_{k-1}^{\tau}$ and $\hat{\mathbf{P}}_{k-1}^{\tau}$, yielding $\hat{\mathbf{x}}_{k,1:1}^{\tau}$ and $\hat{\mathbf{P}}_{k,1:1}^{\tau}$ $(1 \le \tau \le K)$;

Step 2: use measurements at sensor 2 to update $\hat{\mathbf{x}}_{k,1:1}^{\tau}$ and $\hat{\mathbf{P}}_{k,1:1}^{\tau}$, yielding $\hat{\mathbf{x}}_{k,1:2}^{\tau}$ and $\hat{\mathbf{P}}_{k,1:2}^{\tau}$ $(1 \le \tau \le K)$. Repeat this process until step N.

Step N: , use measurements at sensor N to update $\hat{\mathbf{x}}_{k,1:N-1}^{\tau}$ and $\hat{\mathbf{P}}_{k,1:N-1}^{\tau}$, yielding $\hat{\mathbf{x}}_{k,1:N}^{\tau}$ and $\hat{\mathbf{P}}_{k,1:N}^{\tau}$ $(1 \le \tau \le K)$.

$\hat{\mathbf{x}}_{k,1:N}^{\tau}$ and $\hat{\mathbf{P}}_{k,1:N}^{\tau}$ are the estimates of the target state and covariance matrix at time k, i.e. $\hat{\mathbf{x}}_{k}^{\tau} = \hat{\mathbf{x}}_{k,1:N}^{\tau}$, and $\hat{\mathbf{P}}_{k}^{\tau} = \hat{\mathbf{P}}_{k,1:N}^{\tau}$. Therefore (7) can be computed as

$$p(\mathbf{x}_k^{\tau}|\mathbf{Y}_1^k, \ldots, \mathbf{Y}_N^k) = N(\mathbf{x}_k^{\tau}|\hat{\mathbf{x}}_{k,1:N}^{\tau}, \hat{\mathbf{P}}_{k,1:N}^{\tau})$$

In the following we will show how to update $\hat{\mathbf{x}}_{k,1:s-1}^{\tau}$ and $\hat{\mathbf{P}}_{k,1:s-1}^{\tau}$ by using measurements at sensor s, i.e. $\mathbf{y}_{s,k}$.

With $\hat{\mathbf{x}}_{k,1:s-1}^{\tau}$ and $\hat{\mathbf{P}}_{k,1:s-1}^{\tau}$, the probability density of $\mathbf{x}_k^{\tau}$ conditioned on measurements at the first s-1 sensors is approximated as

$$\begin{aligned}
&p(\mathbf{x}_k^{\tau}|\mathbf{Y}_1^k, \ldots, \mathbf{Y}_{s-1}^k, \mathbf{Y}_s^{k-1} \ldots, \mathbf{Y}_N^{k-1}) \\
&\qquad = N(\mathbf{x}_k^{\tau}|\hat{\mathbf{x}}_{k,1:s-1}^{\tau}, \hat{\mathbf{P}}_{k,1:s-1}^{\tau})
\end{aligned}$$

Thus $\hat{\mathbf{x}}_{k,1:s-1}^{\tau}$ and $\hat{\mathbf{P}}_{k,1:s-1}^{\tau}$ $(1 \le \tau \le K)$ contain all the statistical information in $\mathbf{Y}_1^k, \ldots, \mathbf{Y}_{s-1}^k, \mathbf{Y}_s^{k-1} \ldots, \mathbf{Y}_N^{k-1}$. The probability density of $\mathbf{x}_k^{\tau}$ conditioned on measurements at the first s sensors is thus

$$\begin{aligned}
&p(\mathbf{x}_k^{\tau}|\mathbf{y}_{s,k}, \mathbf{Y}_1^k, \ldots, \mathbf{Y}_{s-1}^k, \mathbf{Y}_s^{k-1} \ldots, \mathbf{Y}_N^{k-1}) \\
&= p(\mathbf{x}_k^{\tau}|\mathbf{y}_{s,k}, \hat{\mathbf{x}}_{k,1:s-1}^{1}, \ldots, \hat{\mathbf{x}}_{k,1:s-1}^{K}) \\
&= \sum_{\boldsymbol{\varepsilon}_s} p(\mathbf{x}_k^{\tau}|\boldsymbol{\varepsilon}_s, \mathbf{y}_{s,k}, \hat{\mathbf{x}}_{k,1:s-1}^{\tau}) p(\boldsymbol{\varepsilon}_s|\mathbf{y}_{s,k}, \hat{\mathbf{x}}_{k,1:s-1}^{1}, \ldots, \hat{\mathbf{x}}_{k,1:s-1}^{K}) \\
&\approx N(\mathbf{x}_k^{\tau}|\hat{\mathbf{x}}_{k,1:s}^{\tau}, \hat{\mathbf{P}}_{k,1:s}^{\tau})
\end{aligned} \tag{15}$$

where

$$\begin{aligned}
\hat{\mathbf{x}}_{k,1:s}^{\tau} &= \sum_{i_s=0}^{n_s} \alpha_{i_s}^{\tau} \tilde{\mathbf{x}}_{k,1:s-1}^{\tau}(i_s) \\
\hat{\mathbf{P}}_{k,1:s}^{\tau} &= \sum_{i_s=0}^{n_s} \alpha_{i_s}^{\tau} \Big\{ \tilde{\mathbf{P}}_{k,1:s-1}^{\tau}(i_s) + (\tilde{\mathbf{x}}_{k,1:s-1}^{\tau}(i_s) - \hat{\mathbf{x}}_{k,1:s}^{\tau}) \\
&\qquad \times (\tilde{\mathbf{x}}_{k,1:s-1}^{\tau}(i_s) - \hat{\mathbf{x}}_{k,1:s}^{\tau})^T \Big\}
\end{aligned} \tag{16}$$

$\tilde{\mathbf{x}}_{k,1:s-1}^{\tau}(i_s)$ and $\tilde{\mathbf{P}}_{k,1:s-1}^{\tau}(i_s)$ are the results of updating $\hat{\mathbf{x}}_{k,1:s-1}^{\tau}$ by suing measurement $\mathbf{y}_{s,k}(i_s)$. Similar to the P-MSJPDA, KF is not applicable to compute the statistical quantities above owing to the nonlinearity of the measurement equation in PMSR. A sequential UKF for computing $\tilde{\mathbf{x}}_{k,1:s-1}^{\tau}(i_s)$ and $\tilde{\mathbf{P}}_{k,1:s-1}^{\tau}(i_s)$ with $\mathbf{y}_{s,k}(i_s)$, $\hat{\mathbf{x}}_{k,1:s-1}^{\tau}$, and $\hat{\mathbf{P}}_{k,1:s-1}^{\tau}$ is proposed in this paper and shown in the appendix.

In (15), $\boldsymbol{\varepsilon}_s$ is an association event that assigns each measurement at sensor s to a target or claims it as clutter, as shown in section II. $\alpha_{i_s}^{\tau}$ is the probability of associating $\mathbf{y}_{s,k}(i_s)$ to target τ, and is the summation of the posterior probabilities of all the association events $\boldsymbol{\varepsilon}_s$ in which $\mathbf{y}_{s,k}(i_s)$ is assigned to target τ, i.e.

$$\alpha_{i_s}^{\tau} \propto \sum_{\boldsymbol{\varepsilon}_s} p(\boldsymbol{\varepsilon}_s|\hat{\mathbf{x}}_{k,1:s-1}^{1}, \ldots, \hat{\mathbf{x}}_{k,1:s-1}^{K}, \mathbf{y}_{s,k}) \tag{17}$$

where

$$\begin{aligned}
&p(\boldsymbol{\varepsilon}_s|\hat{\mathbf{x}}_{k,1:s-1}^{1}, \ldots, \hat{\mathbf{x}}_{k,1:s-1}^{K}, \mathbf{y}_{s,k}) \\
&\quad \propto p(\mathbf{y}_{s,k}|\boldsymbol{\varepsilon}_s, \hat{\mathbf{x}}_{k,1:s-1}^{1}, \ldots, \hat{\mathbf{x}}_{k,1:s-1}^{K}) \\
&\quad \propto \prod_{j=1}^{L} p(\mathbf{y}_{s,k}(i_s^{(j)})|\mathbf{Z}_{\tau,i_s}^{(j)}, \hat{\mathbf{x}}_{k,1:s-1}^{\tau^{(j)}})
\end{aligned} \tag{18}$$

$p(\mathbf{y}_{s,k}(i_s)|\mathbf{Z}_{\tau,i_s}, \hat{\mathbf{x}}^{\tau}_{k,1:s-1})$ is the predicted measurement likelihood and can also be computed by using the procedure in the appendix.

Similar to the P-MSJPDA, in order to compute the association probabilities $\alpha^{\tau}_{i_s}$, the optimal JPDA enumerates all the association events $\boldsymbol{\varepsilon}_s$, which is NP-hard. Still, many association events only have very small probabilities and contribute little to the solution, thus the m-best association events with the m-largest probabilities are utilized instead, which results in a practical and near optimal approximation method. Suppose $\boldsymbol{\varepsilon}^{(1)}_s, \boldsymbol{\varepsilon}^{(2)}_s, \ldots, \boldsymbol{\varepsilon}^{(m)}_s$ are the m-best association events, thus (17) becomes

$$\alpha^{\tau}_{i_s} \propto \sum_{1\le i\le m} p(\boldsymbol{\varepsilon}^{(i)}_s|\hat{\mathbf{x}}^{1}_{k,1:s-1}, \ldots, \hat{\mathbf{x}}^{K}_{k,1:s-1}, \mathbf{y}_{s,k}) \tag{19}$$

Finding the m-best association events in this subsection is a typical m-best 2-D assignment problem, which can be solved optimally in polynomial time. Assigning a cost to each of the association events $\boldsymbol{\varepsilon}_s$ with its generalized likelihood ratio, i.e.

$$c(\boldsymbol{\varepsilon}_s) = \prod_{j=1}^{L} \frac{p(\mathbf{y}_{s,k}(i^{(j)}_s)|\mathbf{Z}^{(j)}_{\tau,i_s}, \hat{\mathbf{x}}^{\tau^{(j)}}_{k,1:s-1})}{V_s} \tag{20}$$

and denoting Θ as the association event space which contains all the feasible association events $\boldsymbol{\varepsilon}_s$, the m-best 2-D assignment problem is casted in the following

$$\begin{aligned}
\boldsymbol{\varepsilon}^{(1)}_s &= \arg\min_{\boldsymbol{\varepsilon}_s\in\Theta}\{c(\boldsymbol{\varepsilon}_s)\}\\
\boldsymbol{\varepsilon}^{(2)}_s &= \arg\min_{\boldsymbol{\varepsilon}_s\in\Theta\setminus\boldsymbol{\varepsilon}^{(1)}_s}\{c(\boldsymbol{\varepsilon}_s)\}\\
&\vdots\\
\boldsymbol{\varepsilon}^{(m)}_s &= \arg\min_{\boldsymbol{\varepsilon}_s\in\Theta\setminus\varepsilon^{(n)}_s,\ n=1,2,\ldots,m-1}\{c(\boldsymbol{\varepsilon}_s)\}
\end{aligned} \tag{21}$$

(21) can be solved efficiently by an m-best 2-D assignment algorithm described in [46] with the worst case complexity of $O(mL^4)$, where L is the number of two-tuples in $\boldsymbol{\varepsilon}_s$. This complexity can further be reduced to $O(mL^3)$ with some optimization steps [46].

We need to perform this m-best 2-D assignment in each step. The overall complexity is $O(mNL^3)$, which is better than the m-best $(N+1)$-D assignment case, since there are no relaxation iterations in 2-D assignment. If we take into account the complexity of the computation of the assignment cost, which is $(K+1)\sum_{s=1}^{N} n_s$ in this subsection, the S-MSJPDA well outperforms its parallel counterpart in computation time.

IV. SIMULATION

In this section we will compare the performance of P-MSJPDA and S-MSJPDA in an FM-based PMSR scenario through simulations. We consider a simulation setup shown is figure 2.

Three FM transmitters are used with the carrier frequencies of 93.1 MHz, 90.9 MHz and 99.9 MHz respectively.

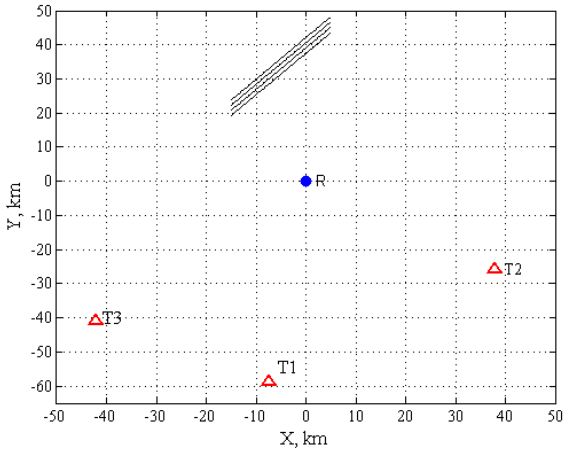

FIGURE 2. Sketch of the simulation scenario.

Four targets fly parallel over the surveillance region from $k = 1$ s to $k = 50$ s with the same initial velocities of $\mathbf{v}^{\tau}(k) = [200, 244.1]^T$ m/s, $\tau = 1, 2\ldots, 4$, and they are about 2 km to each other. In this case the bistatic range and Doppler frequency of the four targets are similar to each other, so both gating and clustering cannot separate the four targets, and then the multi-sensor multi-target tracking problem holds. The relative positions of the transmitters and the receiver, and the trajectories of the four targets are depicted in figure 2, which reveals the real distribution of three FM broadcasting stations in northwest China. The measurement noise follows a Gaussian distribution for bistatic range and Doppler frequency. We set the deviation of the bistatic range to 1000 m, and that of the Doppler frequency to 1 Hz, typical values for FM based passive radar. Under this setup, the four parallel targets in figure 2 cannot be resolved in the bistatic range domain because of the poor range resolution of FM signals. However, they can usually be resolved in the Doppler frequency domain given the excellent Doppler frequency resolution. We thus assume the four targets are resolved. Since the track initiating is not within the scope of this paper, we set the initial state of each track as the true state plus some random noise. Gating and clustering are performed to reduce the computational complexity. It is noted that the same gating and clustering procedures are used in both tracking methods.

We set the detection probability P_{D} and the number of clutter at each sensor per scan as 0.8 and 50 respectively. 100 independent trials are conducted. The root mean square position error (RMSE) of each target is given as

$$\varsigma_{\tau}(k) = \frac{1}{\sqrt{M}}\sqrt{\sum_{i=1}^{M}[\sigma^{i}_{\tau}(k)]^2} \tag{22}$$

where M is the number of Monte Carlo trails, and $\sigma^{i}_{\tau}(k)$ is the position error of target τ at time k corresponding to the i-th trails. The RMSEs of target 1 and 4 are shown in figure 3. It can be seen that the RMSE achieved by P-MSJPDA is close to the true assignment case, however S-MSJPDA degrades

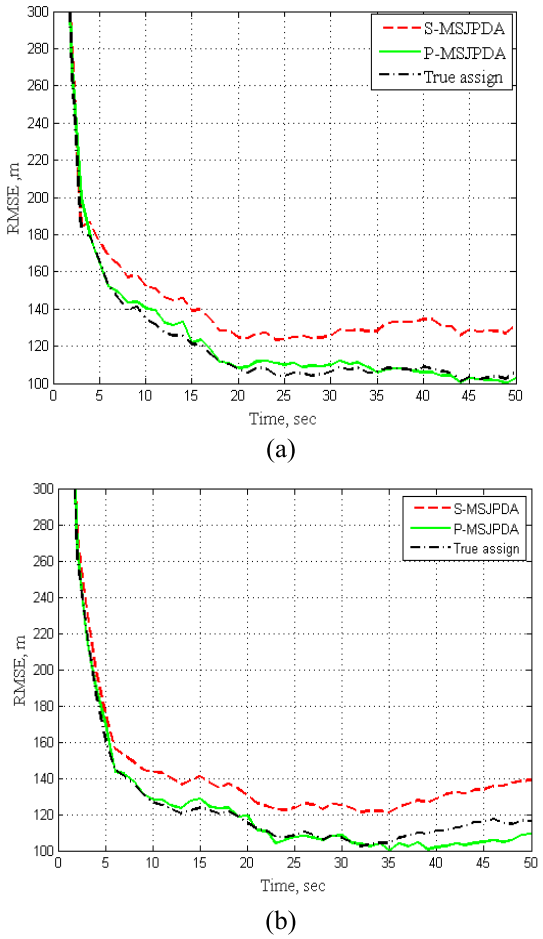

FIGURE 3. RMSEs of target 1and 2. (a) Target 1, (b) target 2.

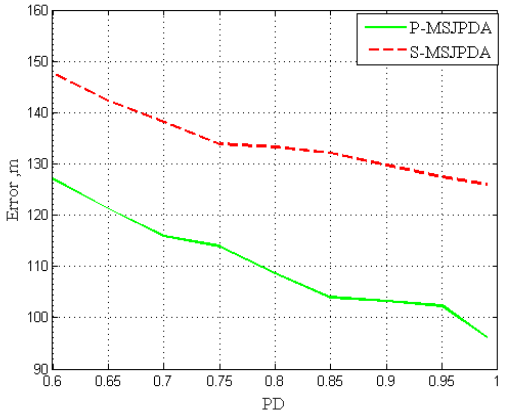

FIGURE 4. Tracker accuracy versus detection probability 50 clutters each sensor per scan.

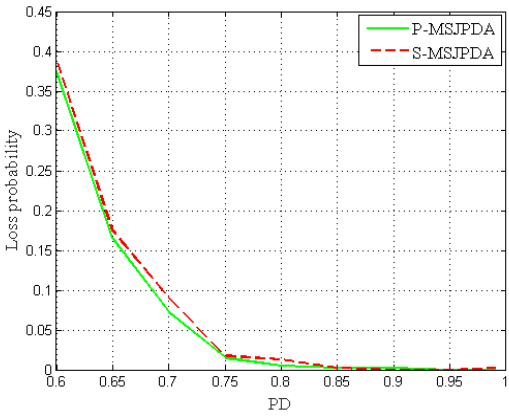

FIGURE 5. Loss probability versus detection probability. 50 clutters each sensor per scan.

slightly. For P-MSJPDA, the converged RMSEs of the two targets are blew 120 m. For S-MPJPDA, the converged RMSEs are between 120 m and 140 m. This is due to the fact that the S-MSJPDA only considers measurements from one sensor per step, and the assignment result will affect that of the next step. For example, if a target is assigned with a dummy measurement or a measurement from another target at sensor s, the updated target state at step s will have a poor quality, which is not good for the assignment of the next step. Fortunately, the RMSE degradation of S-MSJPDA is quite small compared to the surveillance region size.

In the following we will test the performance of the two tracking methods in terms of position accuracy, loss probability and running time versus detection probability and clutter density. We average $\varsigma_\tau(k)$ over time$k$ and target index τ to denote the position accuracy, i.e. $\varsigma = \frac{1}{4}\sum_{\tau=1}^{4}[\frac{1}{50}\sum_{k=1}^{50}\varsigma_\tau(k)]$. Furthermore, we use a strategy similar to that in [38] to report the loss of a target. That is, for each target, if the dummy measurement has the largest association probability for successive four scans, or the target gate is larger than a certain threshold, the target is declared lost. We take the averaging loss probabilities over the four targets as the loss probability of the tracking method. Finally, we run all the simulations on a PC with four 3.3-GH Intel processors, and use the averaging running time over the M Monte Carlo trails to examine the running time of the two tracking methods.

We first study the performance of the two tracking methods versus the detection probability P_{D}. We set the number of clutters at each time instant per sensor as 50. For each P_{D}, 100 independent trials are conducted. The results are displayed in figure 4, 5 and table I. Figure 4 depicts the position accuracy of the two tracking methods. It is seen that the position accuracy of the both methods increases with detection probability P_{D}. This is because more true measurements are available to update the targets as P_{D} increases. The position accuracy of the S-MSJPDA degrades slightly compared to the P-MSJPDA. Figure 5 depicts the loss probabilities of the two methods. It can be seen that the loss probabilities of the both methods decrease with the increase of P_{D} where more true measurements are available. Since the S-MSJPDA only degrades slightly in position accuracy, the loss detection performance of this method is similar to that of the P-MSJPDA. Table I shows the running time of the two tracking methods. It can be seen that the S-MSJPDA is much faster than the P-MSJPDA. This verifies the previous analysis

TABLE 1. Running time versus detection probability.

PD	2-D Assignment, sec	(N+1)-D Assignment, sec
0.6	2.23	34.46
0.65	2.31	33.94
0.7	2.33	32.58
0.75	2.34	30.77
0.8	2.45	30.12
0.85	2.38	26.07
0.9	2.49	22.84
0.95	2.54	19.34
0.99	2.52	17.04

There are 50 clutters at each sensor per scan

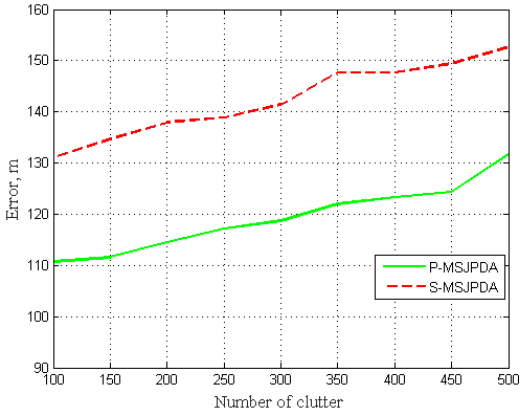

FIGURE 6. Tracker accuracy versus clutter density ($P_D = 0.8$).

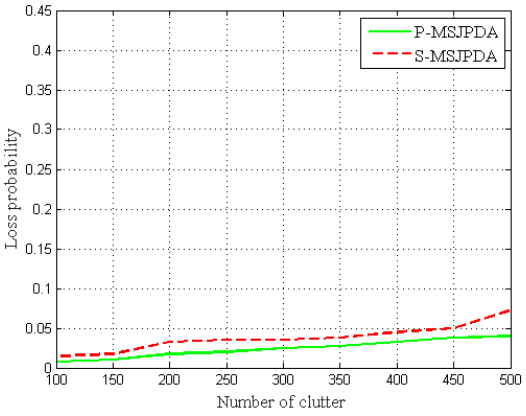

FIGURE 7. Loss probability versus clutter density ($P_D = 0.8$).

TABLE 2. Running time versus clutter density.

Clutter density	2-D Assignment, sec	(N+1)-D Assignment, sec
100	2.72	29.95
150	2.92	30.47
200	3.10	30.52
250	3.27	30.88
300	3.45	30.54
350	3.65	30.51
400	3.87	31.15
450	4.10	31.22
500	4.31	33.21

that the computation of the assignment costs in S-MSJPDA is more efficient. It can also be seen that as P_D increases the S-MSJPDA becomes slow while the P-MSJPDA goes fast. This is because of the nature of the 2-D and S-D assignments as P_D increases [45], [46]. Anyway, the S-MSJPDA is much faster than its parallel counterpart for all P_D tested.

There are 50 clutters at each sensor per scan

We then test the performance of both tracking methods versus the clutter density. We set the detection probability as 0.8. We vary the number of clutter at each sensor per scan from 100 to 500. For each clutter density, 100 independent trials are conducted. The results are displayed in figure 6, 7 and table II. Figure 6 shows the position accuracy of the two tracking methods. It can be seen that the position accuracy of both methods degrades with the increase of the clutter density. However, this degradation is quite small compared with the surveillance region size because of the pre-performing of the gating procedure. It can also be seen that the P-MSJPDA is still slightly better than the S-MSJPDA. Figure 7 displays a similar performance of the both methods in loss probabilities. Table II shows the running time of the two methods. It can be seen that the S-MSJPDA is much faster than the P-MSJPDA. It is noted that since gating and clustering are performed, the performance of both methods only degrades slightly in terms of position accuracy, loss probability, and running time with the increase of clutter density.

We have also tried to reduce the distance between targets to see the behaviors of the two tracking methods and found that the tracks obtained tend to switch to the trajectories of the other targets as their distance decreases especially when it is smaller than 1 km, the deviation of the bistatic range. The closer the targets are to each other, the more frequent the track switch is. This is quite expectable since the measurements from one target may be closer to another target if the distance between the two targets are smaller than the measurement deviation. In this case the measurements will be assigned to a false target and the track switch occurs.

It can be concluded from the above simulations that the S-MSJPDA is much more efficient than the P-MSJPDA in PMSR target tracking, with acceptable degradation in position accuracy and loss probability.

V. EXPERIMENTAL RESULTS

In this section we will apply the S-MSJPDA to an experimental FM-based PMSR for aircraft tracking in real life scene. The distribution of the transmitters and receiver is the same with that shown in figure 2. The signal processing procedure of the radar is shown in figure 8.

The radar is equipped with an 8-element uniform circular antenna array to collect the reference signal and target echoes. Each array element is connected to a digital channelized receiver to resolve signals coming from different FM transmitters. For each transmit-receive pair, the reference signal is extracted by using the beamforming technique.

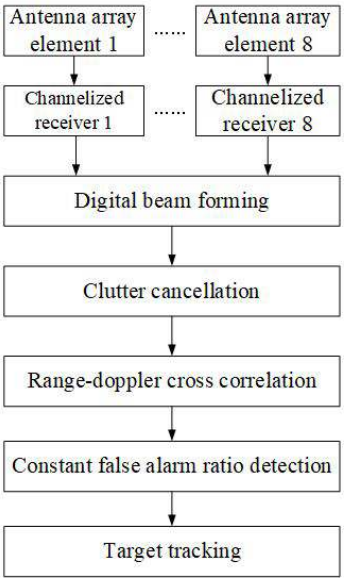

FIGURE 8. Signal processing diagram of the experimental FM-based PMSR.

With the reference signal, clutter cancellation and range-Doppler cross correlation is performed and a constant false alarm ratio (CFAR) procedure is conducted to detect potential targets. If a target is detected on the range-Doppler surface, its bistatic range and Doppler frequency are collected and sent to the target tracking procedure. A comprehensive software is developed based on the compute unified device architecture (CUDA) to perform the beam scanning, clutter cancellation, range-Doppler cross correlation, CFAR detection, and target tracking. The software runs on a Graphic Processing Unit (GPU), thus the radar system can output tracking results at each second. In the target tracking procedure, the m/n logic [22] is designed to initiate new tracks. The S-MSJPDA is developed to maintain the confirmed tracks because of its high efficiency in computation time compared to the P-MSJPDA. The deviation of bistatic range is set to 1000 m. The deviation of Doppler frequency is set to 1 Hz. During the experiment, a lot of tracking results are obtained, among which we only pick out a typical one and depict it in figure 9 by using MATLAB. Figure 9 also displays the ADS-B result. It can be seen that the tracks of the three targets obtained by our radar are rather close to the ADS-B tracks. We take the ADS-B tracks as the real trajectories and use the time average of the absolute difference between the S-MSJPDA tracks and the real trajectories to approximate the RMS track errors. We also count the track length of the three targets. The results are shown in table III. It is seen that the maximum track length maintained by our radar is 75.9 km, and the maintained length of the other tracks exceeds 20 km. The maximum track error is about 0.7 km and the minimum one is 0.45 km, which seam slightly worse than the simulation ones. This may be because we neglect the target's altitude. In addition, we found during the experiment that one of the FM transmitters had poor detection probabilities

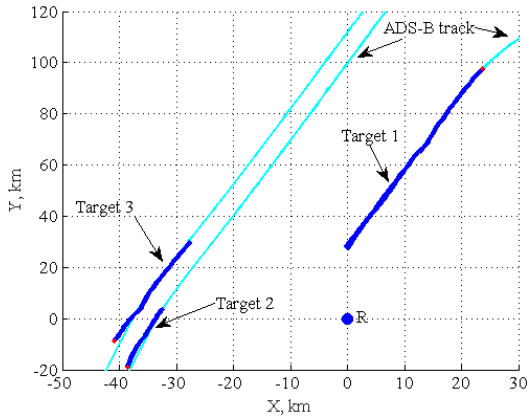

FIGURE 9. Experimental result.

TABLE 3. Track errors and length of the three captured targets.

Track ID	Track length, km	RMS track error, km
1	75.9	0.4381
2	21.75	0.5405
3	46.86	0.7135

over the targets, which also causes the degradation of the position accuracy. It is of limited improvement to include the target altitude into the state vector, since the FM transmitters are not sufficiently distinct in altitudes and in this case it is difficult to estimate a target's altitude with satisfactory accuracy. Adoption of more transmitters and better transmitter-receiver distribution is a reliable way to increase the position accuracy.

VI. CONCLUSION

In this paper we evaluated the behaviors of S-MSJPDA in PMSR target tracking with bistatic range and Doppler frequency measurements. We provided a comprehensive comparison between S-MSJPDA and P-MSJPDA in terms of tracker accuracy, loss probability, and running time. We found from the comparison that the rarely discussed S-MSJPDA is much more efficient than the widely used P-MSJPDA in PMSR, with acceptable degradation in position accuracy and loss probability. We further apply the S-MSJPDA to real life aircrafts tracking using an experimental FM-based PMSR. The tracks of three targets are shown in the paper, among which the maximal track length is up to 75.9km. The track accuracy of the targets is slightly worse than the simulation case, for which the reasons have been analyzed, i.e. neglection of the target's altitude in the tracking system and poor detection probability of one of the three FM transmitters during the experiments. Simulation and experimental results verify that S-MSJPDA has great potentials in target tracking in passive multi-static radar.

APPENDIX

1. **Input**:$\mathbf{y}_{s,k}$ (i_s),$\hat{\mathbf{x}}^{\tau}_{k,1:s-1}$,$\hat{\mathbf{P}}^{\tau}_{k,1:s-1}$, $\mathbf{R}_k$,and $\mathbf{h}_s$;
2. Determine sigma points $\boldsymbol{\chi}_1, \boldsymbol{\chi}_2, \ldots, \boldsymbol{\chi}_Q$ and weights $w_1, w_2, \ldots, w_Q$ to match mean $\hat{\mathbf{x}}^{\tau}_{k,1:s-1}$ and covariance matrix $\hat{\mathbf{P}}^{\tau}_{k,1:s-1}$;

3. Compute the transformed sigma points $\boldsymbol{\xi}_i = \mathbf{h}_s(\boldsymbol{\chi}_i)$;
4. Compute the predicted measurement statistics:

$$\hat{\mathbf{y}}^{\tau}_{s/1:s-1,k} = \sum_{i=1}^{Q} w_i \xi_i$$

$$\hat{\boldsymbol{\Sigma}}^{\tau}_{s/s:s-1,k} = \mathbf{R}_k + \sum_{i=1}^{Q} w_i (\boldsymbol{\xi}_i - \hat{\mathbf{y}}^{\tau}_{s/1:s-1,k})(\boldsymbol{\xi}_i - \hat{\mathbf{y}}^{\tau}_{s/1:s-1,k})^T$$

$$\boldsymbol{\psi}_k = \sum_{i=1}^{Q} w_i (\boldsymbol{\chi}_i - \hat{\mathbf{x}}^{\tau}_{k,1:s-1})(\boldsymbol{\xi}_i - \hat{\mathbf{y}}^{\tau}_{s/1:s-1,k})^T$$

The predicted measurement likelihood is computed as:

$$p(\mathbf{y}_{s,k}(i_s)|\mathbf{Z}_{\tau,i_s}, \hat{\mathbf{x}}^{\tau}_{k,1:s-1}) = N(\mathbf{y}_{s,k}(i_s)|\hat{\mathbf{y}}^{\tau}_{s/1:s-1,k}, \hat{\boldsymbol{\Sigma}}^{\tau}_{s/s:s-1,k})$$

5. Compute the posterior mean and covariance matrix:

$$\tilde{\mathbf{x}}^{\tau}_{k,1:s-1}(i_s) = \hat{\mathbf{x}}^{\tau}_{k,1:s-1} + \boldsymbol{\psi}_k (\hat{\boldsymbol{\Sigma}}^{\tau}_{s/s:s-1,k})^{-1} \times (\mathbf{y}_{s,k}(i_s) - \hat{\mathbf{y}}^{\tau}_{s/1:s-1,k})$$

$$\tilde{\mathbf{P}}^{\tau}_{k,1:s-1}(i_s) = \hat{\mathbf{P}}^{\tau}_{k,1:s-1} - \boldsymbol{\psi}_k (\hat{\boldsymbol{\Sigma}}^{\tau}_{s/s:s-1,k})^{-1} (\boldsymbol{\psi}_k)^T$$

6. **Output**:

$$\tilde{\mathbf{x}}^{\tau}_{k,1:s-1}(i_s), \tilde{\mathbf{P}}^{\tau}_{k,1:s-1}(i_s), p(\mathbf{y}_{s,k}(i_s)|\mathbf{Z}_{\tau,i_s}, \hat{\mathbf{x}}^{\tau}_{k,1:s-1}).$$

REFERENCES

[1] F. Colone, D. W. O'Hagan, P. Lombardo, and C. J. Baker, "A multistage processing algorithm for disturbance removal and target detection in passive bistatic radar," *IEEE Trans. Aerosp. Electron. Syst.*, vol. 45, no. 2, pp. 698–722, Apr. 2009.

[2] C. J. Baker, H. D. Griffiths, and I. Papoutsis, "Passive coherent location radar systems. Part 2: Waveform properties," *IEE Proc. Radar, Sonar Navigat.*, vol. 152, no. 3, pp. 160–168, Jun. 2005.

[3] D. Pastina, F. Colone, T. Martelli, and P. Falcone, "Parasitic exploitation of Wi-Fi signals for indoor radar surveillance," *IEEE Trans. Veh. Technol.*, vol. 64, no. 4, pp. 1401–1415, Apr. 2015.

[4] F. Colone, D. Pastina, P. Falcone, and P. Lombardo, "WiFi-based passive ISAR for high-resolution cross-range profiling of moving targets," *IEEE Trans. Geosci. Remote Sens.*, vol. 52, no. 6, pp. 3486–3501, Jun. 2014.

[5] S. Di Domenico, M. De Sanctis, E. Cianca, P. Colucci, and G. Bianchi, "LTE-based passive device-free crowd density estimation," in *Proc. IEEE Int. Conf. Commun.*, Paris, France, Jul. 2017, pp. 1–6.

[6] S. Bartoletti, A. Giorgetti, M. Z. Win, and A. Conti, "Blind selection of representative observations for sensor radar network," *IEEE Trans. Veh. Technol.*, vol. 64, no. 4, pp. 1388–1400, Jan. 2015.

[7] D. K. P. Tan, H. Sun, Y. Lu, M. Lesturgie, and H. L. Chan, "Passive radar using Global System for Mobile communication signal: Theory, implementation and measurements," *IEE Proc.-Radar, Sonar Navigat.*, vol. 152, no. 3, pp. 116–123, Jun. 2005.

[8] R. Saini and M. Cherniakov, "DTV signal ambiguity function analysis for radar application," *IEE Proc.-Radar, Sonar Navigat.*, vol. 152, no. 3, pp. 133–142, Jun. 2005.

[9] X. He, T. Zeng, and M. Cherniakov, "Signal detectability in SS-BSAR with GNSS non-cooperative transmitter," *IEE Proc.-Radar, Sonar Navigat.*, vol. 152, no. 3, pp. 124–132, Jun. 2005.

[10] H. D. Griffiths and C. J. Baker, "Passive coherent location radar systems. Part 1: Performance prediction," *IEE Proc.-Radar, Sonar Navigat.*, vol. 152, no. 3, pp. 153–159, Jun. 2005.

[11] M. Edrich, A. Schroeder, and F. Meyer, "Design and performance evaluation of a mature FM/DAB/DVB-T multi-illuminator passive radar system," *IET Radar, Sonar Navigat.*, vol. 8, no. 2, pp. 114–122, Feb. 2014.

[12] M. Edrich and A. Schroeder, "Multiband multistatic passive radar system for airspace surveillance: A step towards mature PCL implementations," in *Proc. Int. Conf. Radar*, Adelaide, SA, Australia, Sep. 2013, pp. 218–223.

[13] N. J. Willis, H. D. Griffiths, D. K. Barton, and N. J. Willis, "Air surveillance," in *Advances in Bistatic Radar*. New York, NY, USA: SciTech, 2007, pp. 78–192.

[14] P. E. Howland, D. Maksimiuk, and G. Reitsma, "FM radio based bistatic radar," *IEE Proc.-Radar Sonar Navigat.*, vol. 152, no. 3, pp. 107–115, Jun. 2005.

[15] L. Xiao-Yong, W. Jun, and W. Jue, "Robust direction of arrival estimate method in FM-based passive bistatic radar with a four-element Adcock antenna array," *IET Radar, Sonar Navigat.*, vol. 9, no. 4, pp. 392–400, Apr. 2015.

[16] D. Musicki and B. L. Scala, "Multi-target tracking in clutter without measurement assignment," *IEEE Trans. Aerosp. Electron. Syst.*, vol. 44, no. 3, pp. 877–896, Jul. 2008.

[17] H. Leung, Z. Hu, and M. Blanchette, "Evaluation of multiple target track initiation techniques in real radar tracking environments," *IEE Proc.-Radar, Sonar Navigat.*, vol. 43, no. 4, pp. 246–254, Aug. 1996.

[18] D. Mušicki, "Track score and target existence," in *Proc. 9th IEEE Int. Conf. Inf. Fusion*, Florence, Italy, Jul. 2006, pp. 1–7.

[19] Y. Bar-Shalom, S. S. Blackman, and R. J. Fitzgerald, "Dimensionless score function for multiple hypothesis tracking," *IEEE Trans. Aerosp. Electron. Syst.*, vol. 43, no. 1, pp. 392–400, Jan. 2007.

[20] M. Daun and R. Kaune, "Gaussian mixture initialization in passive tracking applications," in *Proc. 13th Int. Conf. Inf. Fusion*, Edinburgh, U.K., Jul. 2010, pp. 1–8.

[21] S. Blackman and R. Popoli, "Basic methods for data association," in *Design and Analysis of Modern Tracking Systems*. New York, NY, USA: Artech House, 1999, pp. 325–396.

[22] S. S. Blackman, "A maximum likelihood expression for data association," in *Multiple-target Tracking with Radar Applications*. Dedham, MA, USA: Artech House, 1986, pp. 249–280.

[23] Y. Ruan, L. Hong, and D. Wicker, "Analytic performance prediction of feature-aided global nearest neighbour algorithm in dense target scenarios," *IET Radar, Sonar Navigat.*, vol. 1, no. 5, pp. 369–376, Oct. 2007.

[24] Y. Bar-Shalom, "Multiassignment for tracking a large number of overlapping objects," in *Multitarget-Multisensor Tracking: Applications and Advances*. New York, NY, USA: Artech House, 2000, pp. 199–231.

[25] S. Deb, M. Yeddanapudi, K. Pattipati, and Y. Bar-Shalom, "A generalized S-D assignment algorithm for multisensor-multitarget state estimation," *IEEE Trans. Aerosp. Electron. Syst.*, vol. 33, no. 2, pp. 523–538, Apr. 1997.

[26] K. Chang and Y. Bar-Shalom, "Joint probabilistic data association for multitarget tracking with possibly unresolved measurements and maneuvers," *IEEE Trans. Autom. Control*, vol. 29, no. 7, pp. 585–594, Jul. 1984.

[27] S. S. Blackman, "Multiple hypothesis tracking for multiple target tracking," *IEEE Aerosp. Electron. Syst. Mag.*, vol. 19, no. 1, pp. 5–18, Jan. 2004.

[28] J. A. Roecker and G. L. Phillis, "Suboptimal joint probabilistic data association," *IEEE Trans. Aerosp. Electron. Syst.*, vol. 29, no. 2, pp. 510–517, Apr. 1993.

[29] J. A. Roecker, "A class of near optimal JPDA algorithms," *IEEE Trans. Aerosp. Electron. Syst.*, vol. 30, no. 2, pp. 504–510, Apr. 1994.

[30] I. J. Cox and S. L. Hingorani, "An efficient implementation of Reid's multiple hypothesis tracking algorithm and its evaluation for the purpose of visual tracking," *IEEE Trans. Pattern Anal. Mach. Intell.*, vol. 18, no. 2, pp. 138–150, Feb. 1996.

[31] R. P. S. Mahler, "Finite-set measurements," in *Statisical Multisource-Multitarget Information Fusion*. New York, NY, USA: Artech House, 2007, pp. 287–303.

[32] B.-N. Vo, S. Singh, and A. Doucet, "Sequential Monte Carlo methods for multitarget filtering with random finite sets," *IEEE Trans. Aerosp. Electron. Syst.*, vol. 41, no. 4, pp. 1224–1245, Oct. 2005.

[33] B.-N. Vo and W.-K. Ma, "The Gaussian mixture probability hypothesis density filter," *IEEE Trans. Signal Process.*, vol. 54, no. 11, pp. 4091–4104, Nov. 2006.

[34] Z. Fu, P. Feng, F. Angelini, J. Chambers, and S. M. Naqvi, "Particle PHD filter based multiple human tracking using online group-structured dictionary learning," *IEEE Access*, vol. 6, pp. 14764–14778, Mar. 2018.

[35] M. Tobias and A. D. Lanterman, "Probability hypothesis density-based multitarget tracking with bistatic range and Doppler observations," *IEE Proc.-Radar, Sonar Navigat.*, vol. 152, no. 3, pp. 195–205, Jun. 2005.

[36] L. Y. Pao and C. W. Frei, "A comparison of parallel and sequential implementations of a multisensor multitarget tracking algorithm," in *Proc. Amer. Control Conf.*, Seattle, WA, USA, Jun. 1995, pp. 1683–1687.

[37] M. Daun, U. Nickel, and W. Koch, "Tracking in multistatic passive radar systems using DAB/DVB-T illumination," *Signal Process.*, vol. 92, no. 6, pp. 1365–1386, Jun. 2012.

[38] S. Choi, D. F. Crouse, P. Willett, and S. Zhou, "Approaches to Cartesian data association passive radar tracking in a DAB/DVB network," *IEEE Trans. Aerosp. Electron. Syst.*, vol. 50, no. 1, pp. 649–663, May 2014.
[39] S. Y. Fang, S. H. Park, and T. L. Song, "Multitarget tracking in cluttered environment for a multistatic passive radar system under the DAB/DVB network," *EURASIP J. Adv. Signal Process.*, vol. 2017, no. 1, p. 11, Jan. 2017.
[40] X. Lyu, A. Stove, M. Gashinova, and M. Cherniakov, "Ambiguity function of Iridium signal for radar application," *Electron. Lett.*, vol. 52, no. 19, pp. 1631–1633, Sep. 2016.
[41] X. Lyu, A. Stove, M. Gashinova, and M. Cherniakov, "Ambiguity function of inmarsat BGAN signal for radar application," *Electron. Lett.*, vol. 52, no. 18, pp. 1557–1559, Aug. 2016.
[42] A. J. Izenman, "An introduction to Kalman filtering with applications," *Technometrics*, vol. 30, no. 1, pp. 243–244, 1988.
[43] S. Challa, "Filtering theory and non-maneuvering object tracking," in *Fundamentals of Object Tracking*. Cambridge, U.K.: Cambridge Univ. Press, 2011, pp. 22–61.
[44] T. Sathyan, A. Sinha, T. Kirubarajan, M. Mcdonald, and T. Lang, "MDA-based data association with prior track information for passive multitarget tracking," *IEEE Trans. Aerosp. Electron. Syst.*, vol. 47, no. 1, pp. 539–556, Jan. 2011.
[45] R. L. Popp, K. R. Pattipati, and Y. Bar-Shalom, "M-best S-D assignment algorithm with application to multitarget tracking," *IEEE Trans. Aerosp. Electron. Syst.*, vol. 37, no. 1, pp. 22–39, Jan. 2001.
[46] M. L. Miller, H. S. Stone, and I. J. Cox, "Optimizing Murty's ranked assignment method," *IEEE Trans. Aerosp. Electron. Syst.*, vol. 33, no. 3, pp. 851–862, Jul. 1997.

XIAOYONG LYU was born in Henan, China, in 1988. He received the B.S. degree in electronic and information engineering from Zhengzhou University, China, in 2011, and the Ph.D. degree in signal and information processing from Xidian University, China, in 2017. From 2015 to 2017, he studied as a Visiting Research Ph.D. Student with the Microwave Integrated System Laboratory (MISL), University of Birmingham, U.K.

His current research interests include radar signal processing, estimation theory, and multi-sensor data fusion. He is currently a Lecturer with Zhengzhou University.

JUN WANG was born in Guizhou, China, in 1969. He received the B.S., M.S., and Ph.D. degrees in signal and information processing from Xidian University, China, in 1990, 1995, and 2000, respectively, where he is currently a Professor with the National Laboratory of Radar Signal Processing.

His research interests include digital signal processing, radar imagery, and high-speed signal processing.